Title
The ATP-dependent remodeler RSC transfers histone dimers and octamers through the rapid formation of an unstable encounter intermediate

Author
Rowe, Claire Ellen

Publication Date
2010

Peer reviewed|Thesis/dissertation

The ATP-dependent remodeler RSC transfers histone dimers and octamers through the rapid formation of an unstable encounter intermediate

by

Claire E. Rowe

DISSERTATION

Submitted in partial satisfaction of the requirements for the degree of

DOCTOR OF PHILOSOPHY

in

Biochemistry

in the

GRADUATE DIVISION

of the

UNIVERSITY OF CALIFORNIA, SAN FRANCISCO

Acknowledgments

First I would like to thank my advisor Dr. Geeta Narlikar for her scientific insight and patience. My almost 7 years at UCSF would have seemed much longer if not for the support of the entire Narlikar Lab and all of their help and camaraderie. I would also like to thank all of my classmates, especially Erin Quan and Katie Verges. Lastly I would of course like to thank my family: my parents for the unwavering support and confidence and my husband Lin Shao for his support and for giving me the encouragement I needed to finally leave UCSF.

The ATP-dependent remodeler RSC transfers histone dimers and octamers through the rapid formation of an unstable encounter intermediate

by

Claire E. Rowe

Abstract: RSC, an essential chromatin remodeling complex in budding yeast, is involved in a variety of biological processes including transcription, recombination, repair and replication. How RSC participates in such diverse processes is not fully understood. *In vitro*, RSC uses ATP to carry out several seemingly distinct reactions: it repositions nucleosomes, transfers H2A/H2B dimers between nucleosomes and transfers histone octamers between pieces of DNA. This raises the intriguing mechanistic question of how this molecular machine can use a single ATPase subunit to create these varied products. Here, we use a FRET-based approach to kinetically order the products of the RSC reaction. Surprisingly, transfer of H2A/H2B dimers and histone octamers is initiated on a time scale of seconds when assayed by FRET, but formation of stable nucleosomal products occurs on a time scale of minutes when assayed by native gel. These results suggest a model in which RSC action rapidly generates an unstable encounter intermediate that contains the two exchange substrates in close proximity. This intermediate then collapses more slowly to form the stable transfer products seen on native gels. The rapid, biologically relevant time scale on which the transfer products are generated implies that such products can play key roles *in vivo*.

Table of Contents

List of Figures and Tables

Chapter 1

The ATP-dependent remodeler RSC transfers histone dimers and octamers through the rapid formation of an unstable encounter intermediate

Introduction

The packaging of eukaryotic DNA into chromatin introduces complex regulatory controls on DNA replication, transcription, recombination and repair. Chromatin remodeling complexes play critical roles in controlling access to the underlying DNA during these nuclear processes. While many chromatin remodeling complexes are specialized to regulate a particular type of nuclear process, the SWI/SNF family of complexes has more widespread roles. SWI/SNF complexes are involved in directly regulating transcription at diverse promoters, promoting cell cycle progression by regulating exit from G1, S and M phases, and assisting in DNA repair pathways (*1-3*). These observations raise the question of how SWI/SNF complexes can fulfill such diverse biological functions.

The known biochemical properties of SWI/SNF complexes provide some insights into its diverse functions. SWI/SNF complexes contain one core catalytic ATPase subunit and several additional non-catalytic subunits. Unlike other chromatin remodeling complexes, SWI/SNF complexes catalyze many different outputs from the same nucleosomal template. These outputs include products that result from intramolecular rearrangements, such as translationally repositioned nucleosomes and nucleosomes containing DNA loops, as well as products that result from intermolecular component exchange, such as nucleosomes with transferred H2A-H2B dimers and histone octamers (*4-9*). While these multiple outcomes might be expected from an enzyme that enables a variety of different biological processes, they also raise the fundamental question of how the single ATPase motor in SWI/SNF can generate so many different products. It has

been suggested that one way in which SWI/SNF complexes generate diverse outputs is through the formation of a single unstable intermediate that can collapse into different outputs in a context dependent manner (*4, 10*). However, *in vitro,* nucleosomes with transferred histone dimers appear to form much more slowly than repositioned nucleosomes, which raises the question of whether such transfer products are off pathway outcomes (*5*).

Understanding how SWI/SNF generates multiple outputs would be greatly aided by the identification of reaction intermediates. However, this can be challenging if the reaction intermediates are unstable. Here we use FRET-based approaches to identify intermediates and kinetically order three different products generated by RSC, the major SWI/SNF complex in budding yeast. Surprisingly, we find that formation of dimer and octamer transfer products, as detected by FRET, is initiated at a much faster rate than inferred by gel-based assays. These results lead to a two-step model for generation of transfer products: the first step entails the rapid formation of an encounter intermediate, while the second step entails the slow collapse of this intermediate into a stable product. Our results imply that the dimer and octamer transfer products observed *in vitro* occur through the core mechanistic activity of RSC and are therefore feasible and biologically relevant *in vivo* outcomes.

Experimental Procedures

Protein Purification. RSC was purified from the strain BCY211, a kind gift from Brad Cairns, using a TAP-tag on Rsc2 as described previously (*11*). RSC concentration was quantified by SYPRO red staining.

Nucleosome Assembly. Recombinant *Xenopus* histones were purified as described previously (*12*). To generate fluorescently labeled octamers, a cysteine was engineered into H2A at residue 120 and H3 at residue 33. The cysteine-containing histones were labeled with Cy5 maleimide as described previous (*13*). The 601 positioning sequence was modified, as previously described, to contain a Pst1 site 18 bp from one end (*13*). DNA constructs of various lengths were generated using PCR and gel purified before use. Cy3-labeled constructs were made using an end-labeled primer. Primer sequences are available upon request. Nucleosomes were assembled using gradient salt dialysis as described previously (*12*). Nucleomes were then purified away from free DNA and histones using a glycerol gradient.

Native Gel Assays. RSC remodeling reactions were performed at 30°C in reaction buffer containing 50 mM KCl, 30 mM Tris (pH 7.5), 1 mM free $MgCl_2$, 4% glycerol and 0.02% Igepal CA-630. Saturating RSC, 106.5 nM, was used for all reactions. Repositioning reactions contained 7 nM nucleosome substrate. Dimer transfer reactions contained 7 nM nucleosomes with Cy5-labeled H2A and 28 nM core nucleosome. Octamer transfer reactions contained 7 nM nucleosomes with Cy5-labeled H3 and 28 nM 147 bp core 601 positioning sequence DNA. Reactions were initiated with 1 mM ATP-Mg^{2+} and stopped after the time indicated using excess ADP and plasmid DNA as described previously (*13*). Reactions were run on native 5% (v/v) polyacrylamide gels, 29 to 1 acrylamide to bis-acrylamide ratio, in 0.5 X TBE. Gels were scanned using a Typhoon Variable Mode Imager (GE Healthcare) and quantified using ImageQuant (GE Heathcare). Gels were visualized using either the fluorescent labels or SYBR gold (Invitrogen). Percent transfer was calculated as the fraction of the total Cy5 intensity in

the transferred band. The data were fit to a single exponential with the zero-point fixed to the transfer value at time zero using the following equation:

$$p = (a-b)*e^{(-k1*t)} + b$$

where p is the percent transferred, a is the percent transferred at time zero, b is the percent transferred at time infinity and k1 is the rate constant. The data were then normalized from 0 to 1 using the following equation:

$$n = (p-a)/(b-a)$$

where n is the normalized transfer. In Figure 4, the reactions were stopped by adding ADP to a final concentration of 58 mM. ADP uncontaminated by ATP was purchased from Calbiochem, cat# 117105. Reactions stopped with 0.1 units/μL apyrase, Sigma-Aldrich A6410, gave similar results as reactions stopped using ADP.

FRET-based kinetics experiments. FRET assays were conducted using the same reaction conditions as the native gel assays. Fluorescence was measured on an ISS K2 fluorometer. Kinetics were measured as described previously (*13*), with samples excited at 520 nm and spectra collected at Cy3 or Cy5 peak intensity, 567 or 670 nm, respectively. All reactions contained 1 mM free $MgCl_2$ and either 1 mM or 20 μM ATP-Mg^{2+} as indicated in the text. Reactions were initiated by adding ATP-Mg^{2+}. The data were fit to either one or two exponentials using the curve fitting toolbox of MATLAB (The MathWorks). Data were fit to two exponentials using the following equation:

$$i=(a*e^{(-k1*x)})+c-(b*k1/(k1-k2))*(e^{(-k1*x)}-e^{(-k2*x)})+(c/(k1-k2))*(k2*\exp^{(-k1*x)}-k1*\exp^{(-k2*x)})$$

where i is the fluorescence intensity, a is intensity of the starting substrate, b is the intensity of the intermediates, c is the intensity of the final product, k1 is the rate constant for the first phase and k2 is the rate constant for the second phase. The intensity

at time zero, a, was fixed when the data were fit. The intensity at time zero was calculated by measuring the average intensity for 45 s before initiating the reactions and then correcting this value for the dilution that occurred when the reaction was initiated.

Results

RSC creates three distinct products that can be visualized on native gels

It has previously been shown using native gel-based assays that RSC and other SWI/SNF complexes can reposition nucleosomes towards DNA ends, exchange H2A/H2B dimers between nucleosomes and transfer histone octamers between pieces of DNA (*5-7, 14, 15*). We first confirmed that we could analogously visualize these three distinct products with our RSC preparation and nucleosomal constructs. To monitor changes in nucleosome position, histone H3 was labeled with Cy5 on a single cysteine residue introduced at position 33, and octamers containing this histone were assembled on a DNA fragment with 40 bp of flanking DNA on either side of a centrally placed 601 positioning sequence (40-601-40). As expected, RSC repositions these centered nucleosomes, creating a new species with a mobility consistent with end positioned nucleosomes (Figure 1A lanes 1 and 2, Supplementary Figure 1).

To detect dimer transfer, we took advantage of the fact that nucleosomes formed on DNA of different lengths can be resolved on a native gel. To track the histone dimer, H2A was labeled with Cy5 on a single cysteine residue introduced at position 120. Histone octamers containing this labeled H2A were assembled on the 39-601-39 DNA fragment. RSC acts on these nucleosomes in the presence of unlabeled core nucleosomes to generate two Cy5 labeled products (Figure1B lanes 3 and 4, Supplementary Figure 1): a repositioned nucleosome and a core nucleosome. These data

indicate that the H2A/H2B dimer is transferred to the unlabeled core nucleosome as observed previously.

To track octamer transfer, nucleosomes with Cy5-labeled H3 were assembled on the 40-601-40 DNA fragment. These nucleosomes were mixed with a 147 bp fragment of DNA containing the 601 positioning sequence. We find that in the presence of RSC and ATP, a new product appears on the gel that migrates with the same mobility as a core nucleosome (Figure 1C lanes 5 and 6 and Supplementary Figure 1). These data indicate that RSC transfers the Cy5 labeled octamer from the 202 bp DNA to the 147 bp DNA fragment, consistent with previous observations.

A FRET-based approach reveals a rapid initial phase in the transfer of octamers and dimers

While gel-based assays are very powerful in separating out different remodeled products, these assays cannot always identify transient nucleosomal intermediates. To better understand how RSC generates transfer products we searched for reaction intermediates using a FRET-based assay that allows us to track each process individually. All the experiments in this section were done at 20 μM ATP, a subsaturating concentration that made it possible to capture the fast phases of the reactions. Dimer transfer was tracked using two nucleosomes containing differentially labeled histones. Nucleosomes containing Cy5-labeled H2A were mixed with nucleosomes containing Cy3-labeled H3. In this assay, the Cy5-labeled nucleosomes act as a donor of labeled H2A/H2B dimers while the Cy3-labeled nucleosomes acts as a dimer acceptor. When the Cy5-labeled H2A/H2B dimer from the donor nucleosome is

transferred to the acceptor nucleosome containing Cy3-labeled H3, the two fluorophores are brought together, causing an increase in FRET (Figure 2A). To measure FRET efficiency we excited the nucleosomes at the Cy3 absorption maximum and measured Cy5 emission over time. Interestingly, we found that FRET increases in two phases: a rapid phase with a rate constant of 1.9 ± 0.098 min^{-1}, followed by a slower phase with a rate constant of 0.41 ± 0.028 min^{-1} (Table 1). The two phase nature of the reaction is even more clear at 1 mM ATP (Figure 3) where the difference between the rate constants is larger.

To monitor the transfer of octamers from one piece of DNA to another, nucleosomes containing Cy5-labeled H3 were mixed with Cy3-labeled DNA fragments (Figure 2B). In this assay, the Cy5-labeled nucleosome acts as a donor of labeled octamer while the Cy3-labeled DNA acts as an octamer acceptor. Transfer of the labeled octamer from the donor nucleosome to the acceptor DNA brings the two fluorophores into close proximity causing an increase in FRET. Analogous to dimer transfer, we observed that FRET increased in two phases: a rapid phase with a rate constant of 0.66 ± 0.062 min^{-1}, followed by a slower phase with a rate constant of 0.082 ± 0.015 min^{-1} (Table 1).

Repositioning occurs more quickly than either dimer or octamer transfer

Previous work using native gel-based assays has suggested that nucleosomes with transferred dimers are formed more slowly than repositioned nucleosomes (*5*). To test whether we observe the same phenomenon using our FRET-based assay, we compared the rates of repositioning to that of dimer and octamer transfer. We examined the kinetics of nucleosome repositioning using histone octamers containing Cy5-labeled H3

assembled on a Cy3–labeled DNA fragment containing the 601 positioning sequence flanked by 55 bp of linker DNA on one end. The resulting end-positioned nucleosomes start out with high FRET efficiency that decreases as the nucleosome is repositioned. The decrease in FRET was measured by following the unquenching of Cy3 fluorescence over time.

Comparing the rate of repositioning with that of dimer and octamer transfer is complicated by the fact that transfer reactions are intermolecular reactions between two substrates while repositioning is an intramolecular reaction with a single substrate. In all the reactions, RSC is saturating and in excess of total substrate concentration to ensure that the second substrate in the transfer reactions does not inhibit the remodeling reaction. To further control for the effects of the second substrate the rate of dimer transfer was compared to the rate of repositioning in the presence of core nucleosomes. We found that, at 20 μM ATP, the rate of repositioning is too fast to measure using manual mixing. However, under these conditions we are able to estimate a lower limit on the rate of repositioning to be 9 min^{-1} (Table 1). Based on this limit the fast phase of dimer transfer is at least 5-fold slower than the fast phase of repositioning. Thus although a fast phase is present in the dimer transfer reaction, the repositioning reaction still occurs at a faster rate.

Similarly, the rate of repositioning in the presence of core DNA was too fast to accurately measure and a lower limit on the rate of 9 min^{-1} was also estimated (Table 1). When the rate of octamer transfer is compared to the rate of repositioning in the presence of core DNA, the fast phase of octamer transfer is at least ten-fold slower than the fast phase of repositioning (Table 1). We also noticed that when DNA was added to

the repositioning reaction, there was an additional slower phase in the repositioning kinetics. This slower phase could reflect an additional decrease in FRET caused by the transfer of the Cy5-labeled octamer to the unlabeled core DNA.

The formation of the octamer transfer and dimer exchange intermediates observed by FRET precedes the formation of the stable transferred products observed by native gel

The two phases seen in the FRET kinetics experiments could either represent (i) two populations of nucleosomes that are converted at different rates or (ii) the rapid formation of an intermediate that is converted more slowly to the final product. To further explore these two models, we measured the kinetics of the two transfer reactions using a native gel assay. For dimer exchange at 1 mM ATP, we find that the product seen on the native gel are formed at least 150-fold more slowly than the fast phase seen in the FRET reactions (Figure 3A, Table 1). Also, by FRET, 52% of the change occurs in the fast phase, whereas by gel if a fast phase is present no more than 9% of the change occurs in that phase. When octamer transfer is examined by native gel we do not find any evidence for a fast phase. In fact, octamer transfer products are formed at least 300-fold more slowly in the gel assay than the fast phase observed by FRET (Figure 3B, Table 1). The absence of a large fast phase in the gel-based assays rules out the first model. Together with the fast phase observed by FRET, these data then strongly suggest the presence of a transient intermediate that is formed very rapidly but cannot survive on a gel.

The rate constant for transfer measured in the native gel assay is similar to the rate of the second phase observed by FRET for both dimer and octamer transfer (Figure3, Table 1). This consistent with that this slower phase represents the transition from a transient intermediate to a stable product that is visible on the native gel.

Formation of stable transfer products requires continuous ATP-dependent activity by RSC

Previous work examining octamer transfer has shown that ATP hydrolysis is necessary for the formation of the octamer transfer product (*6, 7*). Additionally it has been shown that the acceptor DNA must be present during ATP hydrolysis. When ATP-dependent nucleosome remodeling was allowed to occur in the absence of acceptor DNA and acceptor DNA was then added after removal of ATP no octamer transfer was observed (*7*). To further investigate if the ATP requirement is specific for the formation of the unstable transfer intermediate we took advantage of our ability to temporally separate the two steps of the transfer reaction. We stopped RSC reactions after most of the fast phase was completed but before the products of dimer or octamer transfer had accumulated. We then used a gel-based assay to determine if stable transferred products could be detected. To stop the reactions, we used excess ADP, which, when added before RSC, is able to completely block repositioning (data not shown). Addition of ADP after 3 minutes prevented the formation of stable transfer products as did the addition of apyrase, which hydrolyzes ATP (Supplemental Figure 2). These results indicate that formation of both the transient intermediate and the stable products require the ATP dependent activity of RSC.

Discussion

Previous work has suggested that SWI/SNF complexes generate an unstable reaction intermediate that contains disrupted histone-DNA contacts (*4, 6, 16, 17*). It has also been proposed that SWI/SNF complexes generate and inter-convert products with different regions of DNA exposed via the formation of such an intermediate (*4-7, 10*). Our results add to this reaction framework by capturing, for the first time, a transient reaction intermediate generated during the octamer and dimer transfer reactions catalyzed by the major SWI/SNF complex in budding yeast, RSC. As discussed below, we hypothesize that this intermediate entails a close encounter between the two exchange substrates and is formed after the disruption of histone-DNA contacts (Figure 5).

Comparison of the FRET-based data and gel-based data suggests that dimer exchange and octamer transfer occur via at least two steps: (i) a fast step in which the histones from the donor nucleosome are brought in close vicinity of the acceptor nucleosome or DNA to generate an unstable intermediate species, and (ii) a slow step in which this unstable species is converted to a stable nuclesome containing histone components deriving from the donor nucleosome. There are two extreme models to explain these observations. We discuss these models in the context of octamer transfer, but a similar analysis would apply to the dimer exchange reaction. In the first model, dissociation of the donor DNA from the histone octamer and association of acceptor DNA with the histone octamer are coupled. The unstable intermediate contains, in close proximity, a donor nucleosome with disrupted histone-DNA contacts and an acceptor DNA (Figure 5A). In such an encounter intermediate, the acceptor DNA could be partially associated

with the exposed regions of the histone octamer in the donor nucleosome. The slow step would then involve complete transfer of the octamer from the donor DNA to the acceptor DNA. This model is consistent with a recent proposal that RSC may generate a nucleosomal intermediate with globally disrupted histone-DNA contacts(*17*). In the second model, dissociation of the donor DNA from the histone octamer and association of acceptor DNA with the histone octamer occur in two separate steps (Figure 5B). The unstable intermediate contains only the histone octamer from the donor nucleosome in close proximity to the acceptor DNA, while the donor DNA is completely removed in a prior step. The slow step would then involve association of the donor DNA with the histone octamer to form a stable nucleosomal complex. In the first model, a slightly positively charged RSC active site could facilitate global histone-DNA disruption as well as accommodate the acceptor DNA. In the second model, the RSC active site has to be compatible with binding a nucleosome as well as the separated histone octamer and DNA, and each imposes very different electrostatic requirements on the RSC active site. In such a case, it is possible, as discussed below, that other RSC subunits participate in binding the different intermediate histone and DNA states.

In both the above models, collapse of the transfer intermediate into a stable nucleosome is not ATP-dependent but the ATP requirement that we observe in Figure 4 arises because, only a small fraction of the disrupted intermediate gets converted to the transfer intermediate in each remodeling cycle. As a result, ATP-dependent RSC activity is necessary to constantly replenish the pool of disrupted intermediate (Figure 5).

By itself, the much slower formation of the stable transfer products, compared to repositioned products, could be interpreted to mean that the transfer products are off-

pathway products. However, the observation that the substrates of the transfer reactions come together much faster suggests that the exchange products can be on-pathway RSC products. Further, the time-scale on which the encounter intermediate is formed is comparable to the *in vivo* time-scales associated with RNA and DNA polymerase translocation on 150 bp of DNA (*18*), raising the possibility that these exchange products can have biologically relevant roles.

Both models (Figure 5) raise the possibility that RSC has binding sites for more than one nucleosomal or DNA substrate. These additional binding sites may be provided by non-catalytic RSC subunits. Precedence for such a mechanism comes from previous work on the SWR and SWI/SNF complexes that identified specific subunits required for dimer transfer (*19, 20*). These subunits are believed to facilitate efficient dimer transfer by directly binding to H2A/H2B dimers. Although a homologous subunit in RSC is not readily apparent, it is possible that one of RSC's many non-catalytic subunits may be involved in binding additional substrates to facilitate transfer. Alternatively, it is possible that RSC lacks any subunits specialized in binding other substrates. In this case, RSC function may be regulated by other chromatin factors that might bias RSC towards forming predominantly dimer exchange or octamer transfer products.

References

1. Cao, Y., Cairns, B. R., Kornberg, R. D., and Laurent, B. C. (1997) Sfh1p, a component of a novel chromatin-remodeling complex, is required for cell cycle progression, *Mol Cell Biol 17*, 3323-3334.
2. Fyodorov, D. V., and Kadonaga, J. T. (2001) The many faces of chromatin remodeling: SWItching beyond transcription, *Cell 106*, 523-525.
3. Becker, P. B., and Horz, W. (2002) ATP-dependent nucleosome remodeling, *Annu Rev Biochem 71*, 247-273.
4. Narlikar, G. J., Phelan, M. L., and Kingston, R. E. (2001) Generation and interconversion of multiple distinct nucleosomal states as a mechanism for catalyzing chromatin fluidity, *Mol Cell 8*, 1219-1230.
5. Bruno, M., Flaus, A., Stockdale, C., Rencurel, C., Ferreira, H., and Owen-Hughes, T. (2003) Histone H2A/H2B dimer exchange by ATP-dependent chromatin remodeling activities, *Mol Cell 12*, 1599-1606.
6. Lorch, Y., Zhang, M., and Kornberg, R. D. (1999) Histone octamer transfer by a chromatin-remodeling complex, *Cell 96*, 389-392.
7. Phelan, M. L., Schnitzler, G. R., and Kingston, R. E. (2000) Octamer transfer and creation of stably remodeled nucleosomes by human SWI-SNF and its isolated ATPases, *Mol Cell Biol 20*, 6380-6389.
8. Lorch, Y., Cairns, B. R., Zhang, M., and Kornberg, R. D. (1998) Activated RSC-nucleosome complex and persistently altered form of the nucleosome, *Cell 94*, 29-34.
9. Saha, A., Wittmeyer, J., and Cairns, B. R. (2006) Mechanisms for nucleosome movement by ATP-dependent chromatin remodeling complexes, *Results Probl Cell Differ 41*, 127-148.
10. Schnitzler, G., Sif, S., and Kingston, R. E. (1998) Human SWI/SNF interconverts a nucleosome between its base state and a stable remodeled state, *Cell 94*, 17-27.
11. Wittmeyer, J., Saha, A., and Cairns, B. (2004) DNA translocation and nucleosome remodeling assays by the RSC chromatin remodeling complex, *Methods Enzymol 377*, 322-343.
12. Dyer, P. N., Edayathumangalam, R. S., White, C. L., Bao, Y., Chakravarthy, S., Muthurajan, U. M., and Luger, K. (2004) Reconstitution of nucleosome core particles from recombinant histones and DNA, *Methods Enzymol 375*, 23-44.
13. Yang, J. G., Madrid, T. S., Sevastopoulos, E., and Narlikar, G. J. (2006) The chromatin-remodeling enzyme ACF is an ATP-dependent DNA length sensor that regulates nucleosome spacing, *Nat Struct Mol Biol 13*, 1078-1083.
14. Cairns, B. R., Lorch, Y., Li, Y., Zhang, M., Lacomis, L., Erdjument-Bromage, H., Tempst, P., Du, J., Laurent, B., and Kornberg, R. D. (1996) RSC, an essential, abundant chromatin-remodeling complex, *Cell 87*, 1249-1260.
15. Bouazoune, K., Miranda, T. B., Jones, P. A., and Kingston, R. E. (2009) Analysis of individual remodeled nucleosomes reveals decreased histone-DNA contacts created by hSWI/SNF, *Nucleic Acids Res 37*, 5279-5294.

16. Lorch, Y., Maier-Davis, B., and Kornberg, R. D. (2006) Chromatin remodeling by nucleosome disassembly in vitro, *Proc Natl Acad Sci U S A 103*, 3090-3093.
17. Lorch, Y., Maier-Davis, B., and Kornberg, R. D. (2010) Mechanism of chromatin remodeling, *Proc Natl Acad Sci U S A 107*, 3458-3462.
18. O'Farrell, P. H. (1992) Developmental biology. Big genes and little genes and deadlines for transcription, *Nature 359*, 366-367.
19. Wu, W. H., Wu, C. H., Ladurner, A., Mizuguchi, G., Wei, D., Xiao, H., Luk, E., Ranjan, A., and Wu, C. (2009) N terminus of Swr1 binds to histone H2AZ and provides a platform for subunit assembly in the chromatin remodeling complex, *J Biol Chem 284*, 6200-6207.
20. Yang, X., Zaurin, R., Beato, M., and Peterson, C. L. (2007) Swi3p controls SWI/SNF assembly and ATP-dependent H2A-H2B displacement, *Nat Struct Mol Biol 14*, 540-547.

Figure 1: RSC catalyzes (A) movement of the DNA relative to the octamer, (B) transfer of H2A/H2B dimers between nucleosomes and (C) transfer of histone octamers between two pieces of DNA. RSC remodeling reactions were run on native gels and scanned in the Cy5 channel. In the reaction schematic shown below each gel, the yellow star shows the position of the Cy5 label and the length of the DNA template (in bp) is indicated below each substrate. All reactions contained 107 nM RSC, 1 mM ATP and 7 nM Cy5 labeled nucleosome. The reactions shown in B and C contain 28 nM of unlabeled core nucleosomes and free DNA, respectively.

Figure 2: FRET-based assays allow separate measurement of the rate constants for (A) dimer transfer, (B) octamer transfer and (C) repositioning. Each panel shows one representative time course at 20 μM ATP. The data points are shown in red and the fit as a black line. The data in (A), (B) and (C) right panel are best fit by two exponentials whereas the data in (C) left panel are best fit by one exponential (see methods). In the reaction schematic below, Cy3 and Cy5 labels are represented as blue and yellow stars respectively.

Figure 3: Changes in FRET precede the formation of the exchange product as visualized by gel. Reactions containing the nucleosome constructs shown in Figure 2 were run on a native gel. The left panels show a representative gel scanned in the Cy5 channel. The graphs on the right show the corresponding normalized data from the native gel (red data points) and FRET assays (black data points). The rate constant for

dimer exchange as measured in the gel assay was 0.072 ± 0.00012min^{-1}. The rate constant for octamer transfer was 0.034 ± 0.00042 min^{-1}. These rate constants are the average and variation of two separate experiments. Reactions were preformed using 1 mM ATP.

Figure 4: Continuous RSC activity is necessary for formation a stable exchange product. Dimer transfer reactions (A) and octamer transfer reactions (B) using the substrates from Figure 1 at 1 mM ATP were analyzed on a native gel. The left gels show the reaction with no ADP added and the right gels show reactions in which excess ADP was added after 3 min. The gels were scanned in the Cy5 channel. The graph shows the quantification of transfer for the reactions with no ADP added in black and ADP added at 3 min in red. The values for dimer transfer are calculated from three independent experiments; error bars show the standard error of the mean. For octamer transfer one representative experiment is shown. Other experiments where ADP was added at different time points showed the same requirement for ATP (data not shown).

Figure 5: Models for RSC catalyzed octamer transfer. In these schematic the acceptor DNA is shown in blue. A disrupted intermediate is inferred based on previous work (*4, 6, 16, 17*) whereas the encounter intermediate is inferred based on this work. It is assumed that repositioning is limited by the formation of the disrupted intermediate, the fast phase of octamer transfer is limited by the formation of the encounter intermediate,

and formation of the stable transfer product is limited by the conversion of the encounter intermediate. ATP is shown for ATP-dependent steps.

Supplementary Figure 1: Confirming the positions of the gel products. (A) Repositioned nucleosomes have the same gel mobility as end positioned nucleosomes. The nucleosome standards used to confirm the positions of the reaction products are indicated above the corresponding wells. Here we show additional lanes of the gels shown in Figure 1. A small amount of the Cy5 label is consistently retained in the wells as shown. (B) SYBR Gold stained gels showing that the products of the dimer and octamer transfer reactions have the same gel mobility as core nucleosomes.

Supplementary Figure 2: Apyrase blocks the formation of the stable transfer product. RSC reactions using the substrates from Figure 1 at 1 mM ATP were separated on a native gel. The left gel shows the reaction with no apyrase added and the right gel shows the reaction in which apyrase was added after 3 min. The gels were scanned in the Cy5 channel. The graph shows quantification of transfer with no apyrase in blue, with ayprase added at 3 min in red, and ayprase added before the reaction was initiated in black. The use of commercially available of apyrase results in the additional background seen in these gels.

Figure 1:

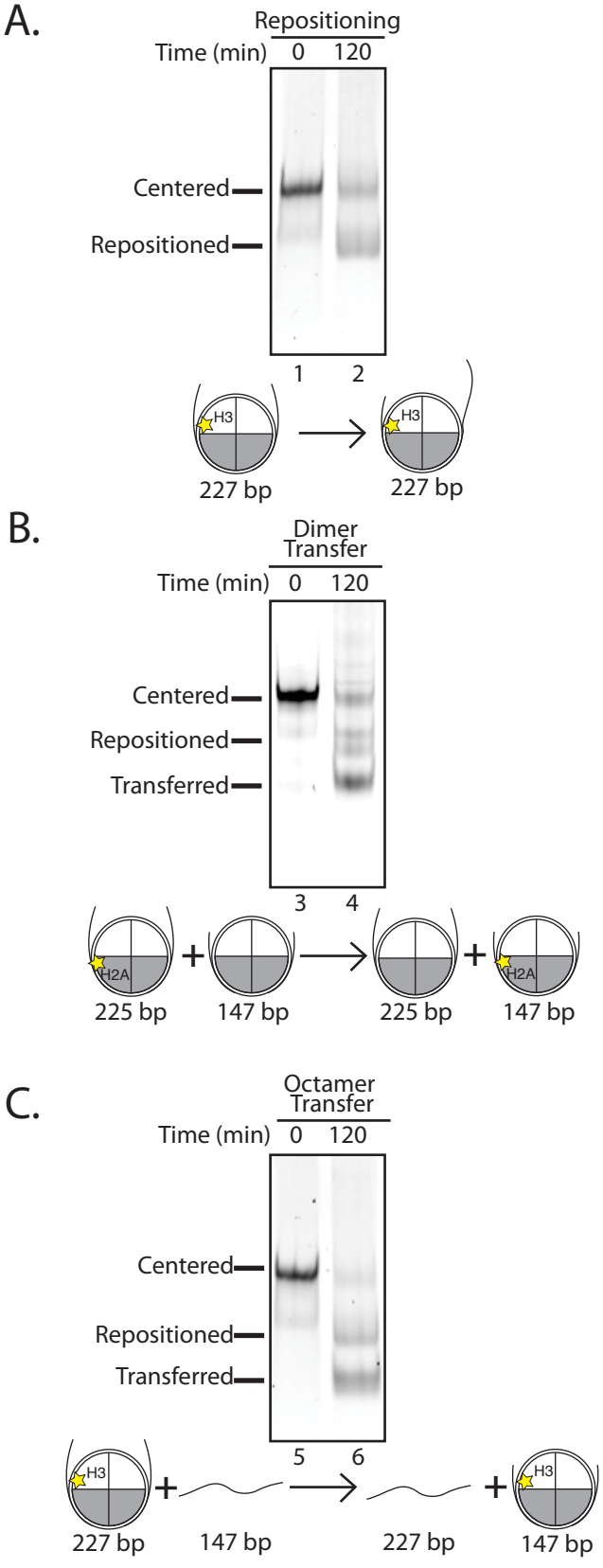
A.
Repositioning
Time (min) 0 120
Centered
Repositioned
1 2
H3
H3
227 bp
227 bp
B.
Dimer Transfer
Time (min) 0 120
Centered
Repositioned
Transferred
3 4
H2A
H2A
225 bp
147 bp
225 bp
147 bp
C.
Octamer Transfer
Time (min) 0 120
Centered
Repositioned
Transferred
5 6
H3
H3
227 bp
147 bp
227 bp
147 bp

Figure 2:

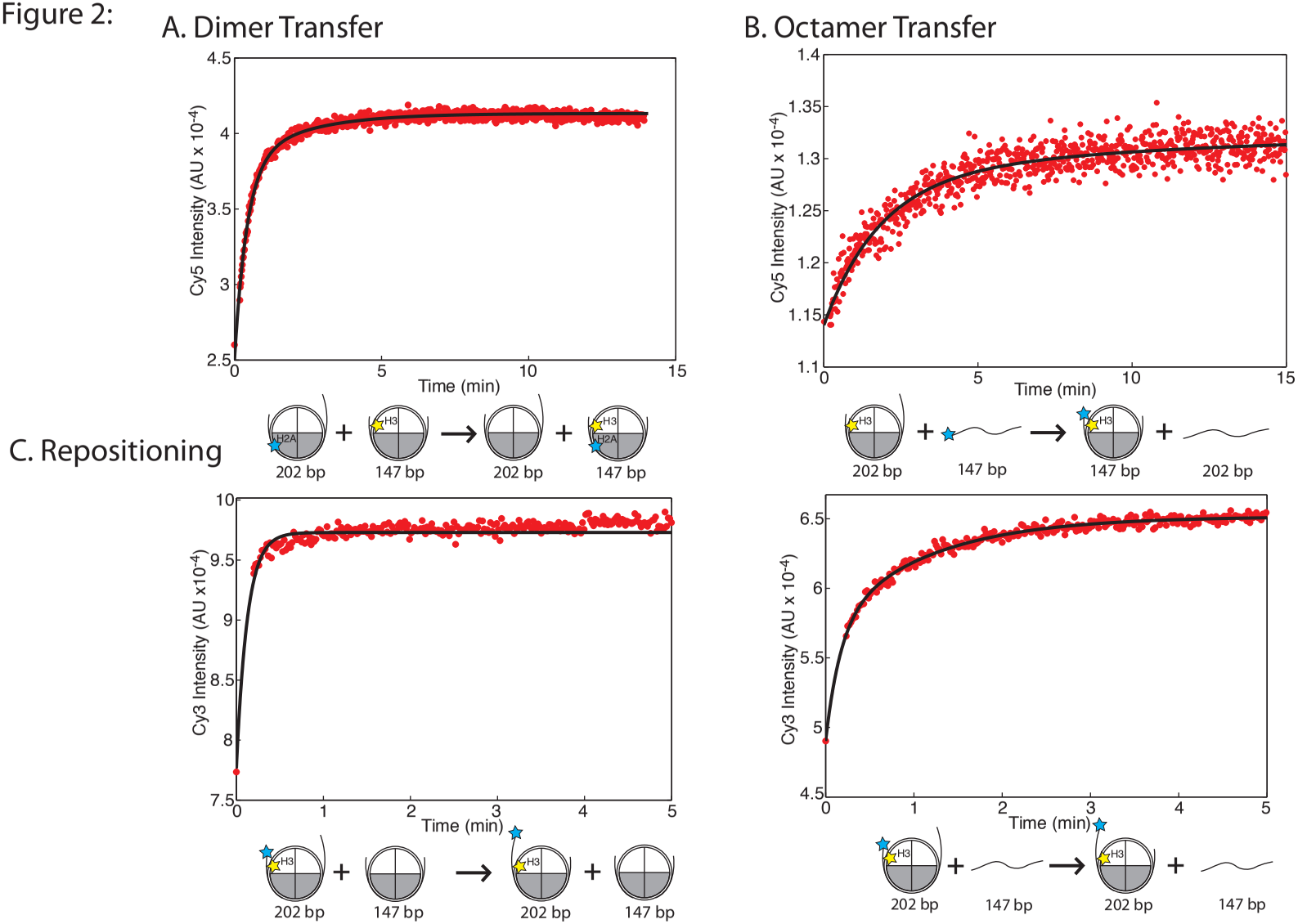
A. Dimer Transfer
Cy5 Intensity (AU x 10-4)
Time (min)
H2A
H3
202 bp
147 bp
202 bp
147 bp
B. Octamer Transfer
Cy5 Intensity (AU x 10-4)
Time (min)
202 bp
147 bp
147 bp
202 bp
C. Repositioning
Cy3 Intensity (AU x10-4)
Time (min)
202 bp
147 bp
202 bp
147 bp
Cy3 Intensity (AU x 10-4)
Time (min)
202 bp
147 bp
202 bp
147 bp

Figure 3:

A. Dimer Transfer

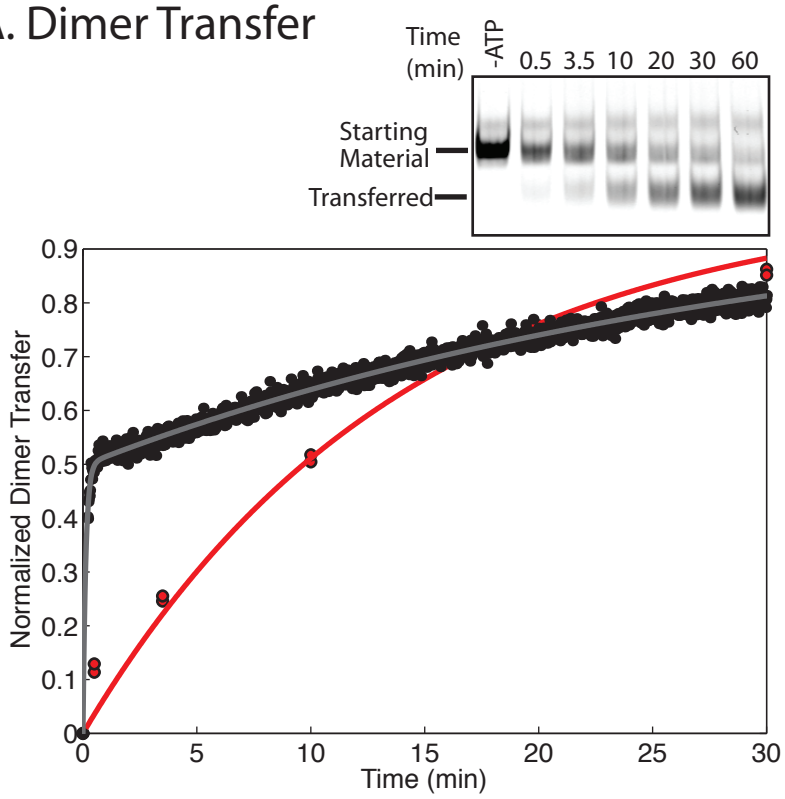

B. Octamer Transfer

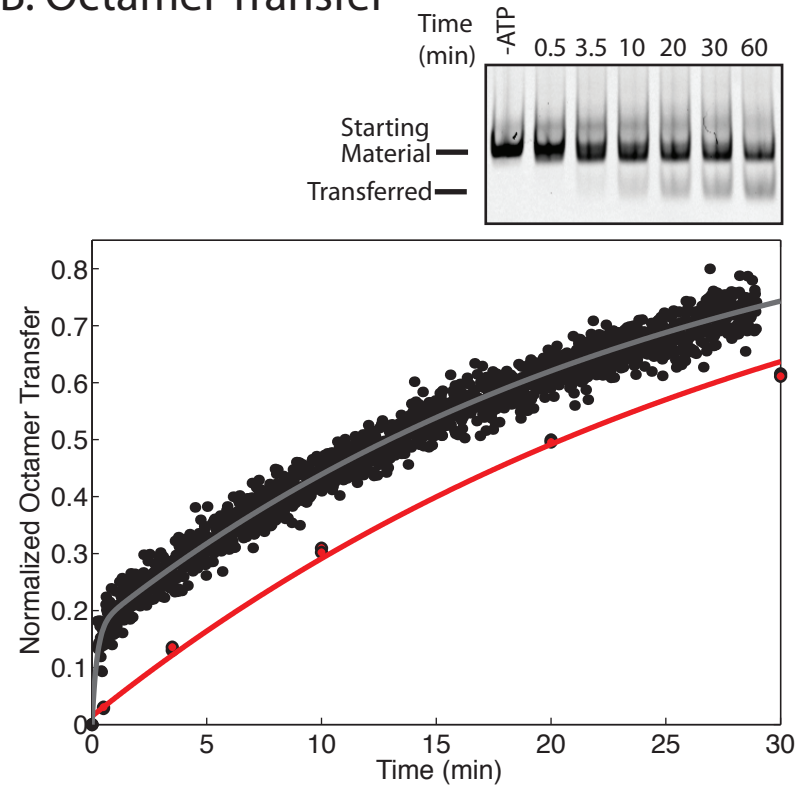

Figure 4:

A. Dimer Transfer

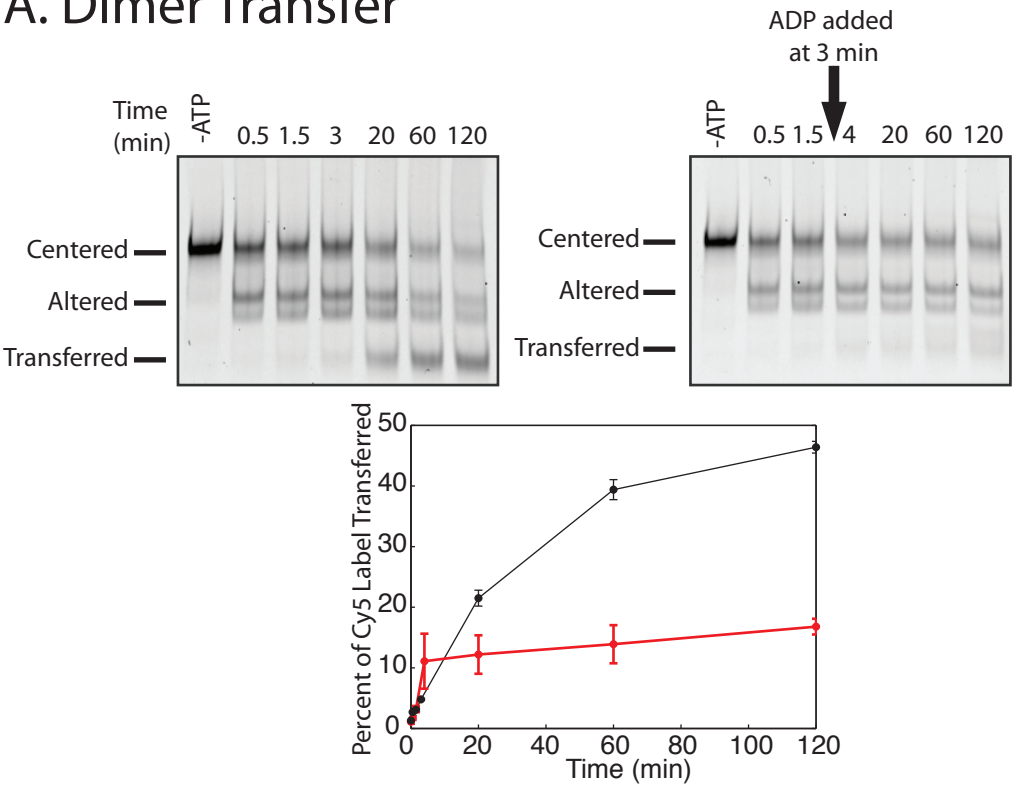

B. Octamer Transfer

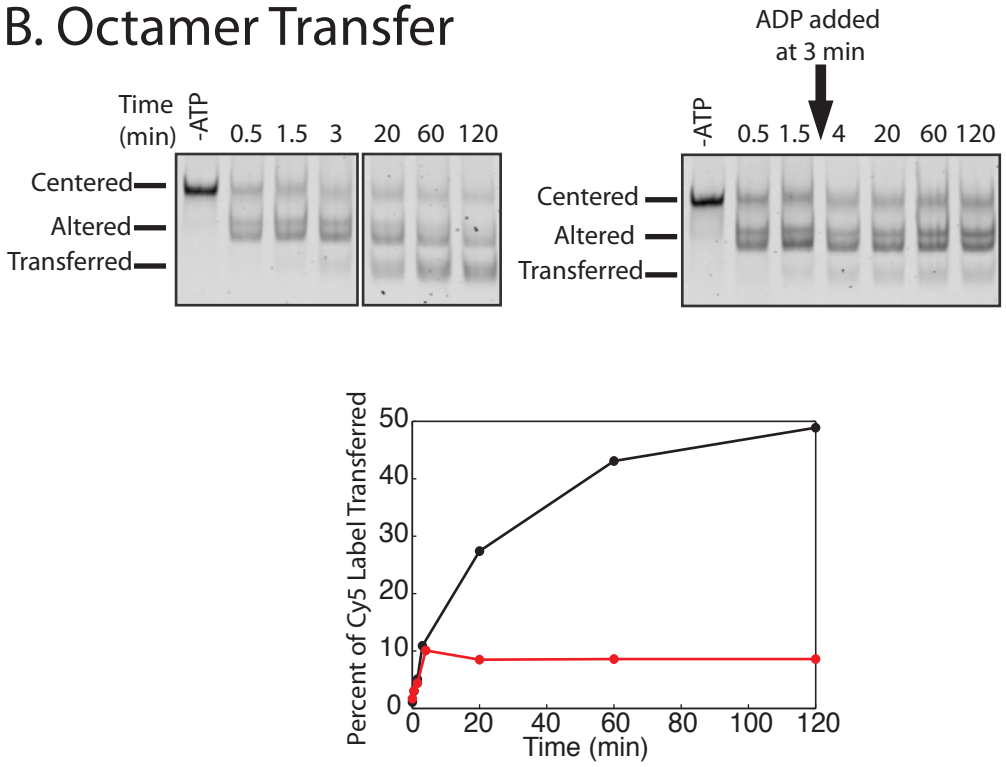

Figure 5:

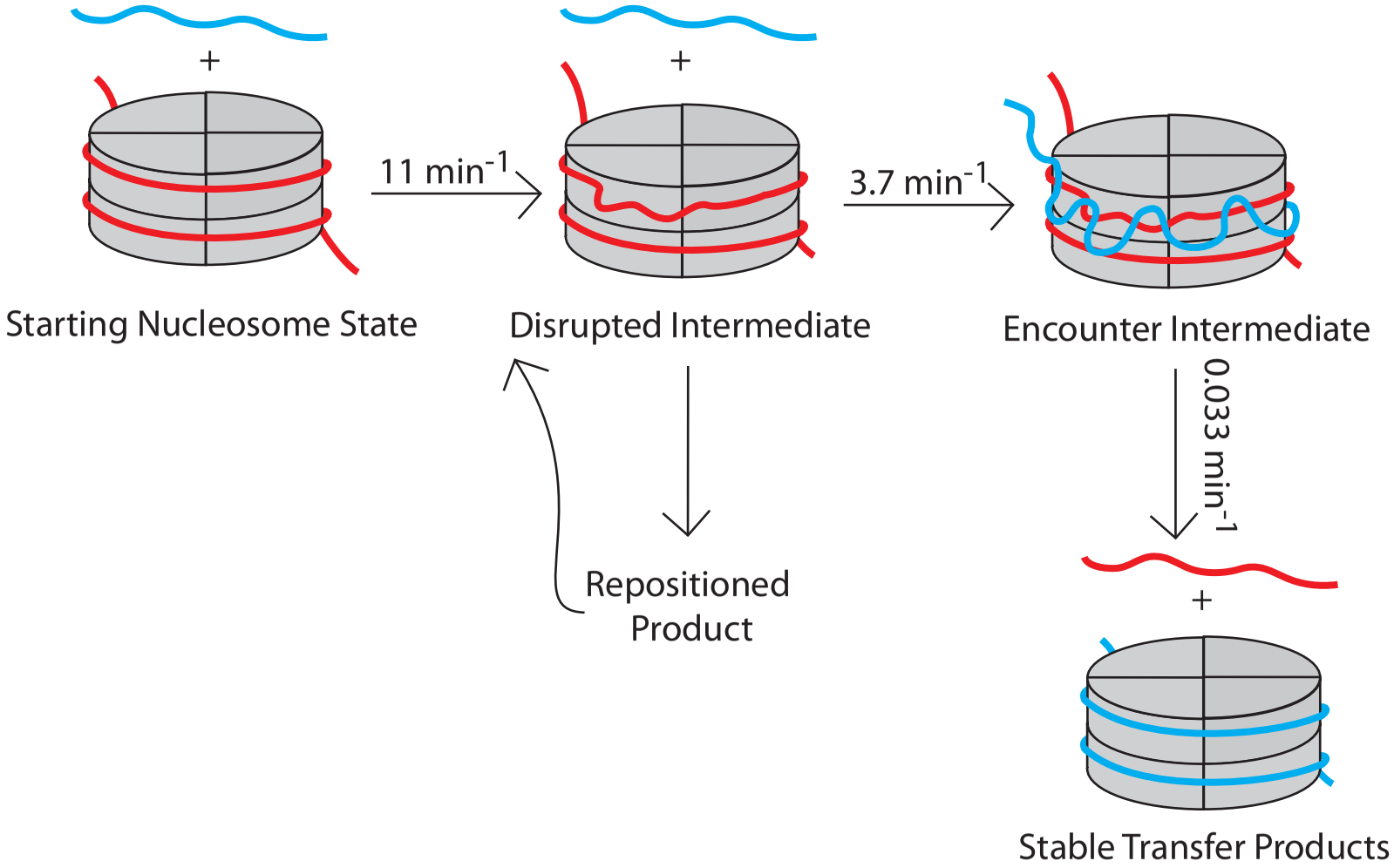
+
11 min-1
+
3.7 min-1
Starting Nucleosome State
Disrupted Intermediate
Encounter Intermediate
0.033 min-1
Repositioned
Product
+
Stable Transfer Products

Table 1. RSC remodeling rate constants

	1 mM ATP		20 μM ATP	
Rate Constants (min^{-1})	k_1	k_2	k_1	k_2
Repositioning Alone	≥ 10		≥ 10	
Dimer Transfer	8.2 ± 0.14	0.027 ± 0.00057	1.9 ± 0.098	0.41 ± 0.028
Repositioning Under Dimer Transfer Reaction Conditions	≥ 10		≥ 9	
Octamer Transfer	3.7 ± 1.4	0.033 ± 0.0084	0.66 ± 0.062	0.082 ± 0.015
Repositioning Under Octamer Transfer Reaction Conditions	≥ 10	0.80 ± 0.017	≥ 9	0.83 ± 0.043

Each value is the average of three independent experiments ± standard error of the mean.
k_1 and k_2 are the rate constants of the first and second phase, respectively.

Supplementary Figure 1:

A. Scanned in the Cy5 channel

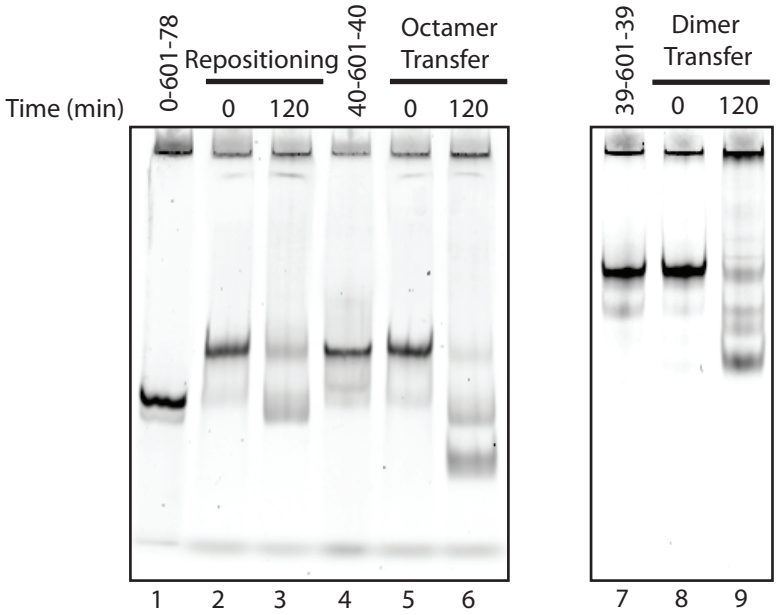

B. Stained with SYBR Gold

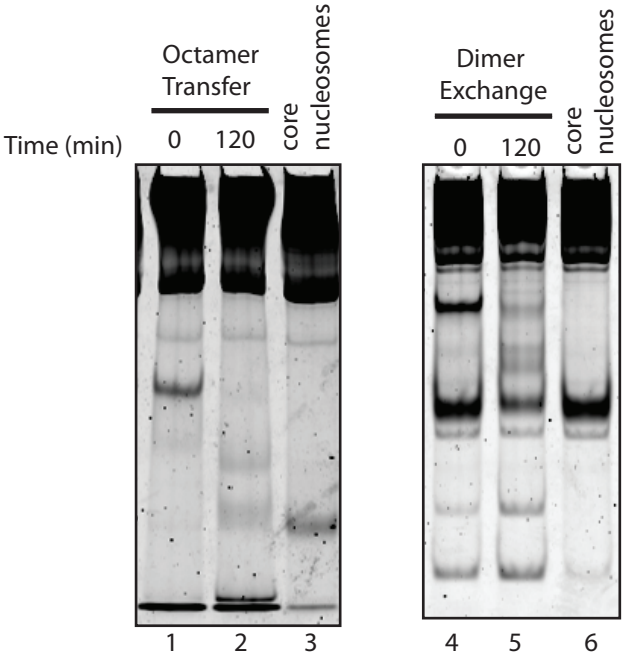

Supplementary Figure 2:

A. Dimer Transfer

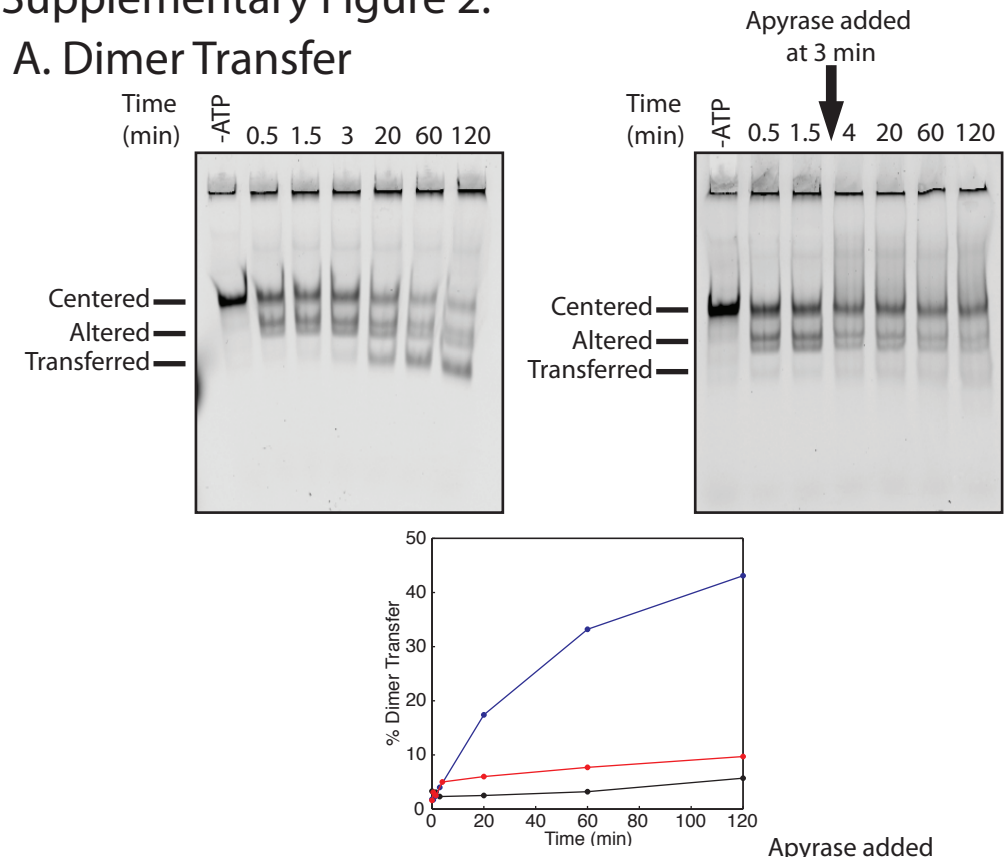

B. Octamer Transfer

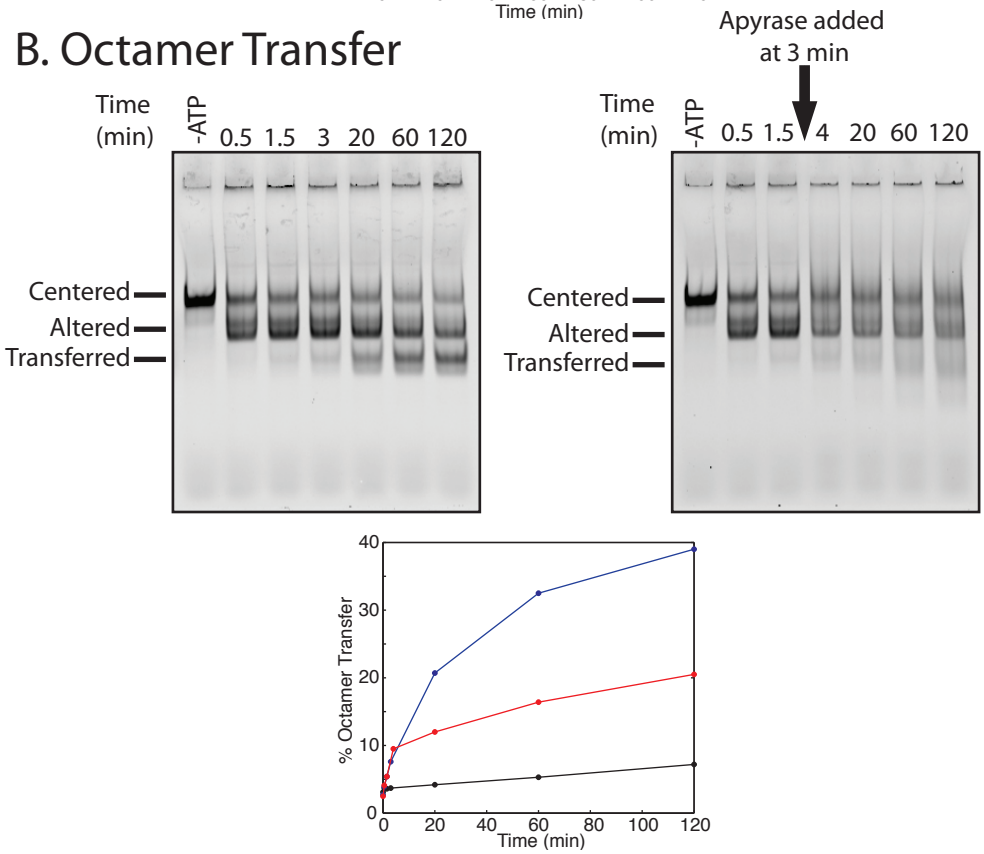

Chapter 2
Unpublished Data

Crosslinking histones H2B and H4

Rationale

Given that dimer transfer is a product of RSC activity, we wondered if removal of the H2A/H2B dimer might be a necessary step in the process of RSC remodeling. Previous work with crosslinked nucleosomes showed that they could still be remodeled (*1*), but in these experiments, crosslinking did not affect the remodeler's ability to remove dimers from the nucleosome. In order to address this question, we sought to specifically crosslink the histone dimer to the tetramer. Precedence for this strategy came from a paper in which the two H3 histones of the octamer were crosslinked through a disulfide bond between the two naturally occurring cysteines at position 120 (*2*).

Placement of Cysteines for Crosslinking

We mutated residues in H2B and H4 to cysteines so that we could crosslink the dimer and tetramer together using a disulfide bond. Two sets of mutants were made: Set 1 consisted of H2B L77C and H4 A76C, while Set 2 consisted of H2B L97C and H4 T71C. These pairs were chosen for having a short distance between these residues in H2B and H4 while having a larger distance between the residue pairs that could crosslink to form homodimers of H2B-H2B or H4-H4. The distances were: for Set 1, 9 and 8 Å between heterodimer pairs with all others more than 23 Å apart, and for Set 2, 5 Å between heterodimer pairs with all others more than 20 Å apart (Figure 1a). The residues were also selected so that the disulfide bond would be close to the surface of the histone octamer.

Crosslinking Methods

Initially, I assembled both sets of histones into octamers under reducing conditions. When I assembled these octamers into nucleosomes in the absence of DTT or any other

reducing agents, I hoped that the cysteines would form disulfide bonds. However, after assembly, most of the H4 remained uncrosslinked. Only a faint band of crosslinked histones were visible when the nucleosomes were examined on an SDS-PAGE gel (data not shown). Next I tried to crosslink the histones in the octamer before assembling them into a nucleosome. The octamers were assembled in the presence of BME, so to remove the reducing agent I dialyzed the octamers over 4 days, diluting the BME to a calculated concentration of 1 fM. Under these conditions I observed minimal crosslinking in the Set 1 octamers. In the Set 2 octamers, about 50% of the H4 were crosslinked. However, two crosslinked bands appeared, most likely H2B-H4 heterodimer and H4-H4 homodimer (data not shown).

To achieve more complete crosslinking, I moved on to crosslinking the histones in their unfolded form. I dissolved lyophilized aliquots of the histones in unfolding buffer containing the reducing agent DTT to minimize the formation of homodimer. Then I mixed the histones and dialyzed them for 2 days against unfolding buffer without reducing agents to a calculated DTT concentration of 700 pM. This resulted in crosslinking of ~70% of the H2B and H4 histones. However, the crosslinking reaction resulted in three products: the desired H2B-H4 crosslinked histones along with equal amounts of crosslinked H2B-H2B and H4-H4 homodimers. When these histones were refolded into octamers, the homodimers remained (Figure 1B lane 1). When Set 2 octamers were assembled into nucleosomes and the protein content of the nucleosomes analyzed on a gel, most of the H4 was crosslinked and homodimers were not present (Figure 1B lane 4). Due to the poor staining of the histones, I was unable to quantify the amount of uncrosslinked H4 present. However, the crosslinking

was complete enough to answer the question of whether removal of the H2A/H2B dimer is necessary for RSC remodeling.

Remodeling of Crosslinked Nucleosomes

REA experiments showed that crosslinking did not affect the rate of remodeling (Figure 2). Crosslinked and uncrosslinked nucleosomes were remodeled with a rate constant of 0.049 min^{-1} and 0.044 min^{-1} respectively. Although the nucleosomes were not completely crosslinked, at least 50% of the nucleosomes were remodeled. This indicated that the remodeling seen is not due to incomplete crosslinking because significantly more than 50% of the H4 in the nucleosomes were crosslinked. Unfortunately, when a new batch of crosslinked nucleosomes was made, they contained a significant amount of uncrosslinked H4 (data not shown), so this result could not be repeated.

Attempts to Increase Crosslinking Efficiency

We tried several approaches to increase the completeness of crosslinking, but none produced significantly better results than simply crosslinking unfolded histones. I tried to purify the heterodimer away from the homodimer using size exclusion columns; however neither the S-75 or S-200 column (G.E. Healthcare) provided sufficient resolution to separate the three species (data not shown). To improve separation, we tried adding a large tag, mCherry (*3*), to H4 followed by a TEV site to allow the tag to be cleaved after separating the crosslinked dimers. Octamers with the mCherry tag at either the C or N terminal could not be assembled into nucleosomes (data not shown). In the end, due to the large number of preparative steps necessary, this strategy did not produce enough material to be useful.

Change in Reaction Endpoint with ATP Concentration

As we were examining the ATP dependence of RSC remodeling, we noticed a strange phenomenon. The endpoint of the RSC reaction increased with increasing ATP. We observed this with all RSC processes: repositioning, dimer transfer, and octamer transfer (Figure 3). This same change in endpoint was observed in gel assays of repositioning and octamer transfer (data not shown). The simplest explanation for the change in endpoint with ATP is that the pool of ATP is being depleted before all of the nucleosomes can be remodeled. However, the addition of more ATP after reaching the endpoint of reactions performed at lower ATP concentrations did not increase the amount of remodeling seen (data not shown). This rules out the simplest model where ATP was simply insufficient.

Another possibility is that RSC loses activity over time. To test this, I monitored the repositioning of nucleosomes by RSC at low ATP concentrations. Once the curve leveled out, I added more RSC to the reaction to see if the addition of fresh RSC could rescue the difference in endpoint (Figure 4a). The addition of RSC did not cause an increase in the amount of repositioning, suggesting that the ATP-dependent changes in endpoint are not due to inactivation of RSC. However, it is possible that the inactivated RSC is bound to the nucleosome, preventing the additional RSC from acting on the nucleosomes. To test this, I preincubated RSC with either nucleosomes or ATP for 1000 seconds before starting the reactions (Figure 4b). RSC was not inactivated by this preincubation. To further test this model, I used subsaturating RSC in octamer transfer reactions. If nucleosomes were being trapped in an inactive RSC complex, then under these conditions only a fraction of the nucleosomes would be trapped, and when more RSC was added the reaction would continue.

Once the endpoint had been reached, the addition of more RSC did not cause any further increase in octamer transfer (Figure 4b).

All of these data taken together suggest that RSC is not being inactivated over time and that sufficient ATP is present. This leaves only changes in nucleosome structure to explain how the endpoint of the reactions changes with ATP concentration. Here we suggest a model in which nucleosomes can enter an unreactive state where RSC is no longer able to remodel them (Figure 5). The model is explained in terms of repositioning but applies to both dimer and octamer transfer. In this model there are two ATP dependent steps to the remodeling process: the creation of disrupted intermediate A and the creation of disrupted intermediate B. Disrupted intermediate A can collapse into the unreactive state, such as a state where RSC binding is prevented. Disrupted intermediate B collapses in an ATP-independent process to form the final repositioned product, which can then be recycled through the remodeling processes. When the ATP concentration is low, the pool of nucleosomes available to become the unreactive side product is larger, thus decreasing the endpoint by trapping more nucleosomes in this unreactive state. When repositioning and octamer transfer were examined at low ATP concentrations using the gel assay, no bands representing the unreactive side product were observed (data not shown). However this does not rule out our model since much of the fluorescence signal is retained in the wells of the gel, and it is also possible that the unreactive side product may have the same mobility as the starting or repositioned nucleosome state.

Change in Cy3 Intensity with RSC binding

It has previously been shown that remodeling enzymes cause an increase in Cy3 fluorescence intensity when they bind to nucleosomes (*4*). RSC also causes an increase Cy3 fluorescence intensity upon binding to a nucleosome or DNA fragment labeled with Cy3. To measure the affinity of RSC for core nucleosomes and a 202 bp DNA fragment, we measured binding curves for these substrates. After the data were fit, the K_d values were found to be 21 nM for core nucleosomes and 38 nM for the 202 bp DNA fragment (Figure 6), significantly higher than previously reported measurements of K_d (*5*). Also, based on this binding data, the 107 nM RSC concentration used in previous remodeling assays would not be saturating.

To ensure that the RSC concentrations used in previous experiments were in fact saturating, I measured repositioning rates over a range of RSC concentrations (Figure 7a). I found that while Cy3 intensity increased with increasing RSC concentration, both before and after the reaction was complete. However the rate of repositioning remained constant (Figure 7b). This shows that the concentration of RSC used in previous remodeling assays was indeed saturating. This leaves open the question why Cy3 intensity continues to increase even when RSC is present at saturating concentrations.

References

1. Boyer, L. A., Shao, X., Ebright, R. H., and Peterson, C. L. (2000) Roles of the histone H2A-H2B dimers and the (H3-H4)(2) tetramer in nucleosome remodeling by the SWI-SNF complex, *J Biol Chem 275*, 11545-11552.
2. Camerini-Otero, R. D., and Felsenfeld, G. (1977) Histone H3 disulfide dimers and nucleosome structure, *Proc Natl Acad Sci U S A 74*, 5519-5523.
3. Shaner, N. C., Campbell, R. E., Steinbach, P. A., Giepmans, B. N., Palmer, A. E., and Tsien, R. Y. (2004) Improved monomeric red, orange and yellow fluorescent proteins derived from Discosoma sp. red fluorescent protein, *Nat Biotechnol 22*, 1567-1572.

4. Racki, L. R., Yang, J. G., Naber, N., Partensky, P. D., Acevedo, A., Purcell, T. J., Cooke, R., Cheng, Y., and Narlikar, G. J. (2009) The chromatin remodeller ACF acts as a dimeric motor to space nucleosomes, *Nature 462*, 1016-1021.
5. Cairns, B. R., Lorch, Y., Li, Y., Zhang, M., Lacomis, L., Erdjument-Bromage, H., Tempst, P., Du, J., Laurent, B., and Kornberg, R. D. (1996) RSC, an essential, abundant chromatin-remodeling complex, *Cell 87*, 1249-1260.
6. Davey, C. A., Sargent, D. F., Luger, K., Maeder, A. W., and Richmond, T. J. (2002) Solvent mediated interactions in the structure of the nucleosome core particle at 1.9 a resolution, *J Mol Biol 319*, 1097-1113.

Figure Legends

Figure 1: Crosslinking histones H2B and H4. (A) The structure of the nucleosomes (*6*) showing the placement of the cysteine residues for Set 2. Histone H3 is shown in green, histone H4 in blue, histone H2A in orange and histone H2B in red. The DNA is shown as a grey ribbon. The residues at the positions where the cysteines were placed are shown as ball and stick models, with H4 T71C shown in cyan and H2B L97C shown in yellow. (B) An SDS-PAGE gel run under oxidizing conditions showing the extent of crosslinking. Crosslinked Set 2 octamers are run in lane 1. Lanes 3 and 5 contain crosslinked H4 T71C and H2B L97C, respectively. Lane 4 contains nucleosomes made using crosslinked Set 2 octamer.

Figure 2: Crosslinked and uncrosslinked nucleosomes are remodeled at the same rate. REA reactions were performed at 1 mM ATP using Hha1 as the restriction enzyme. The data for crosslinked and uncrosslinked nucleosomes are shown in red and blue, respectively, with filled circles for +ATP and open circles for –ATP. The data were normalized and fit to a single exponential, resulting in a rate constant of 0.049 min^{-1} for crosslinked nucleosomes and 0.044 min^{-1} for uncrosslinked nucleosomes.

Figure 3: The endpoint to RSC reactions increases with increasing ATP. FRET curves at the ATP concentrations indicated in the legend showing (A) repositioning, (B) dimer transfer and (C) octamer transfer.

Figure 4: RSC is not inactivated over time. (A) Repositioning FRET curves at 1 μM ATP shown in blue and at 20 μM ATP shown in red. The initial RSC concentration was 107 nM. RSC was added where indicated, roughly doubling and then tripling the initial RSC concentration. (B) Octamer transfer FRET curves. The reaction shown in blue contains 107 nM RSC at 1 mM ATP. RSC and nucleosomes were preincubated for 1000 sec before ATP was added. The reaction shown in red was performed using 107 nM RSC at 20 μM ATP. RSC and ATP were preincubated for 1000 sec before nucleosomes were added. The reaction shown in green was performed using 10.7 nM RSC at 1 mM ATP. RSC was added where indicated, doubling the initial RSC concentration in the reaction. The reaction shown in orange was performed using 10.7 nM RSC at 20 μM ATP; RSC was added where indicated to double the initial RSC concentration in the reaction.

Figure 5: A model for the RSC reaction that accounts for the change in endpoints observed with changing ATP. In this model nucleosome repositioning occurs in two ATP-dependent steps: the transition between the starting nucleosome state and disrupted intermediate A and the transition between disrupted intermediate A and disrupted intermediate B. Disrupted intermediate A can collapse into unreactive side product, while disrupted intermediate B collapses to form the repositioned product.

Figure 6: RSC binding curves. RSC was mixed with substrate in the absence of ATP or Mg^{2+} and the maximum Cy3 intensity was recorded. (A) shows RSC binding to core nucleosomes assembled on Cy3 labeled DNA. (B) shows RSC binding to a 202 bp 601+55 fragment of DNA labeled on both ends with Cy3. The fitted data are shown for each curve.

Figure 7: RSC remodeling rate and changes in Cy3 intensity give different estimates of RSC binding affinity. (A) RSC repositioning reactions were performed at 4 μM ATP. The data for RSC concentration of 35 nM, 70 nM, 107 nM, 200 nM and 324 nM are shown in pink, red, blue, black, and gray, respectively. (B) The repositioning rate constants are shown as red triangles. Cy3 intensity before the addition of ATP:Mg^{2+} and after the reaction was completed are shown as closed and open blue diamonds, respectively.

Figure 1:

A.

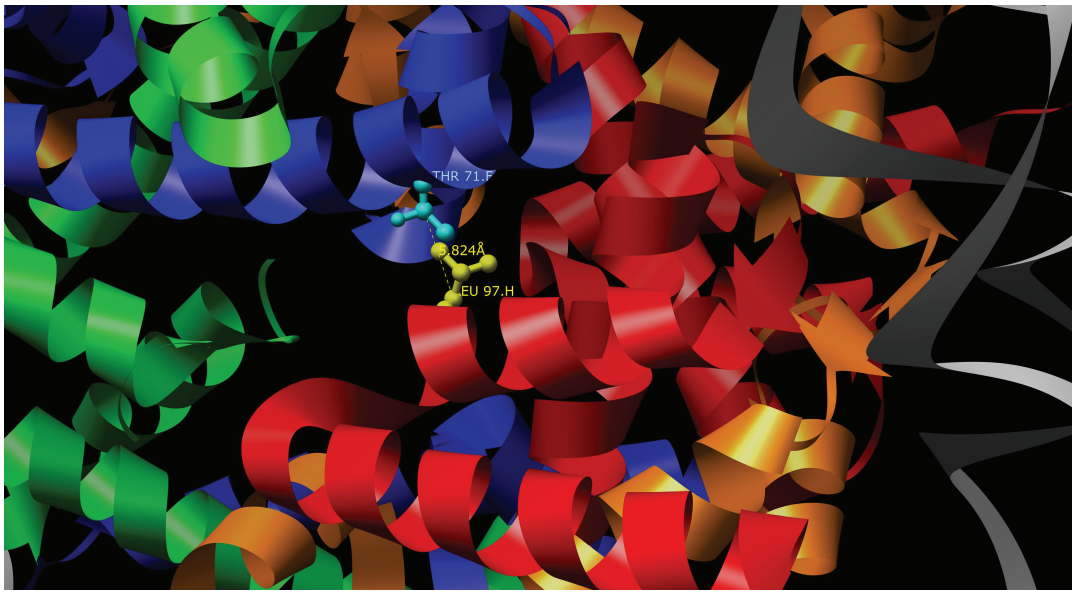
THR 71.F
824Å
EU 97.H

B.

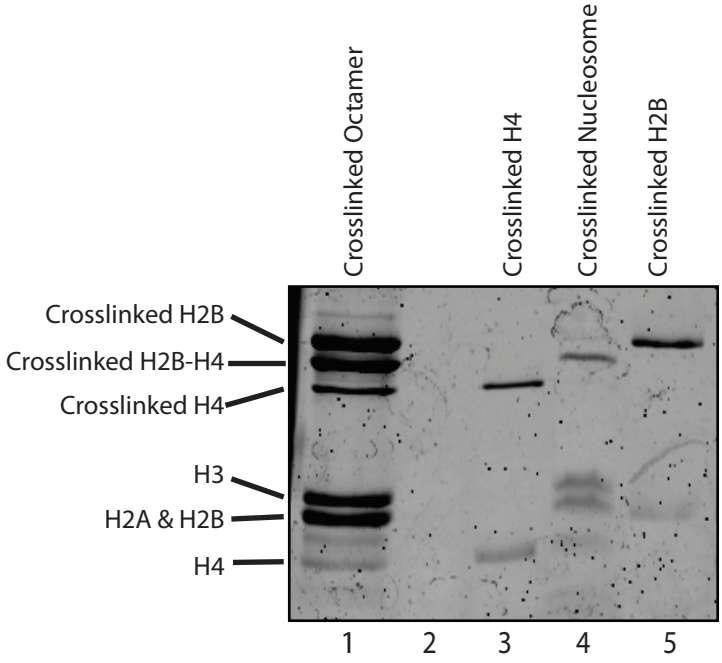
Crosslinked Octamer
Crosslinked H4
Crosslinked Nucleosome
Crosslinked H2B
Crosslinked H2B
Crosslinked H2B-H4
Crosslinked H4
H3
H2A & H2B
H4
1
2
3
4
5

Figure 2:

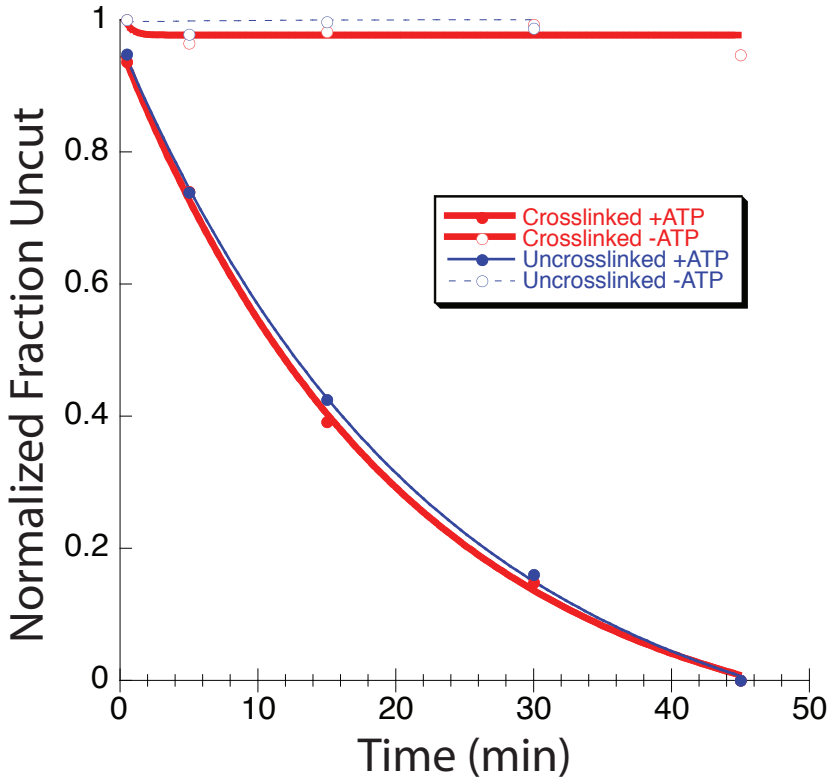
Normalized Fraction Uncut
Time (min)
0
0.2
0.4
0.6
0.8
1
0
10
20
30
40
50
Crosslinked +ATP
Crosslinked -ATP
Uncrosslinked +ATP
Uncrosslinked -ATP

Figure 3:

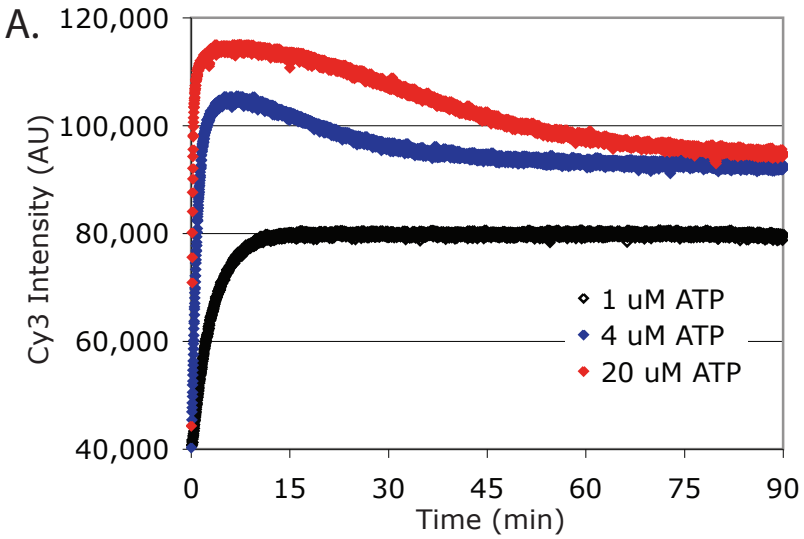
A.
120,000
100,000
80,000
60,000
40,000
Cy3 Intensity (AU)
1 uM ATP
4 uM ATP
20 uM ATP
0
15
30
45
60
75
90
Time (min)

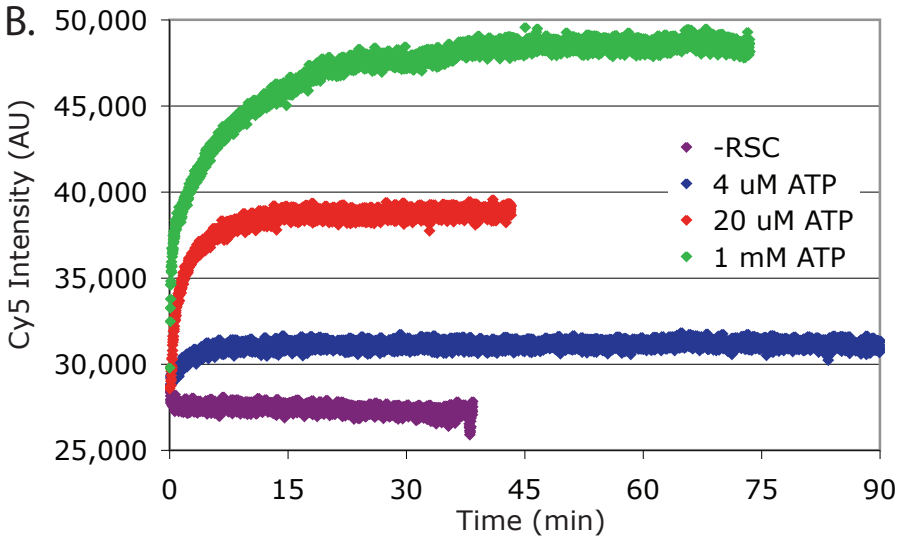
B.
50,000
45,000
40,000
35,000
30,000
25,000
Cy5 Intensity (AU)
-RSC
4 uM ATP
20 uM ATP
1 mM ATP
0
15
30
45
60
75
90
Time (min)

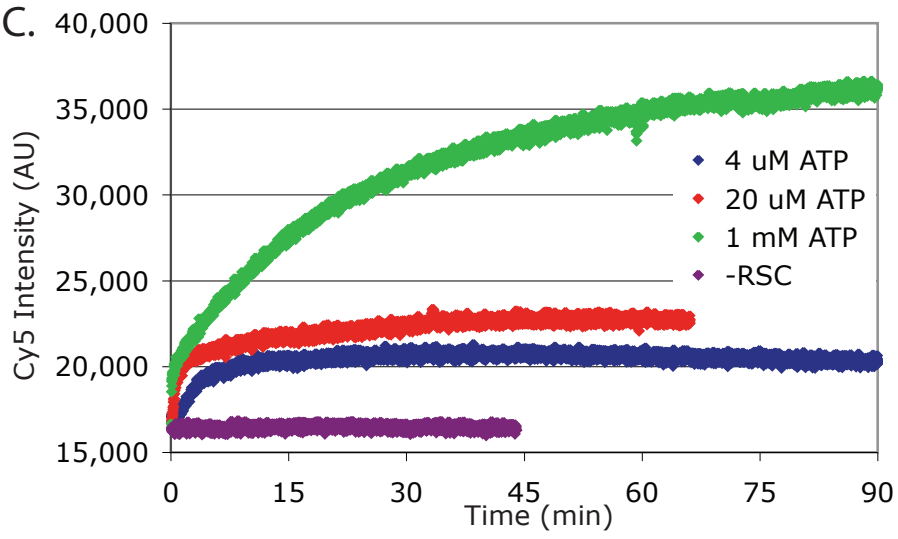
C.
40,000
35,000
30,000
25,000
20,000
15,000
Cy5 Intensity (AU)
4 uM ATP
20 uM ATP
1 mM ATP
-RSC
0
15
30
45
60
75
90
Time (min)

Figure 4:

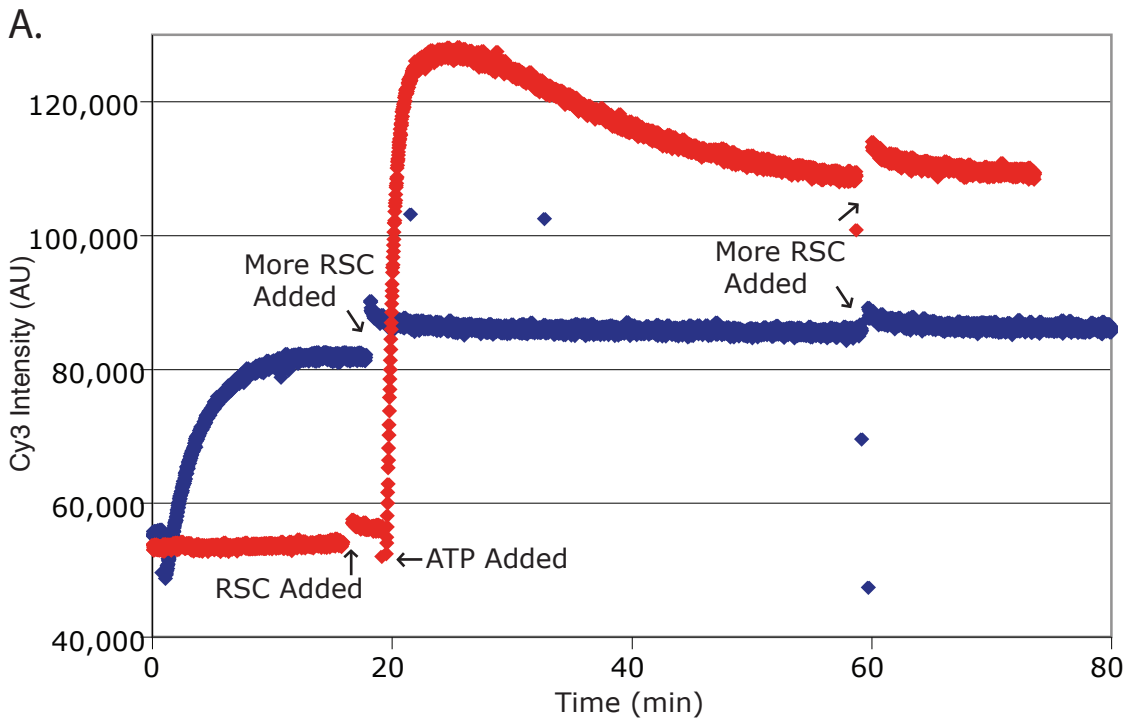
A.
120,000
100,000
80,000
60,000
40,000
Cy3 Intensity (AU)
More RSC Added
More RSC Added
RSC Added
←ATP Added
0
20
40
60
80
Time (min)

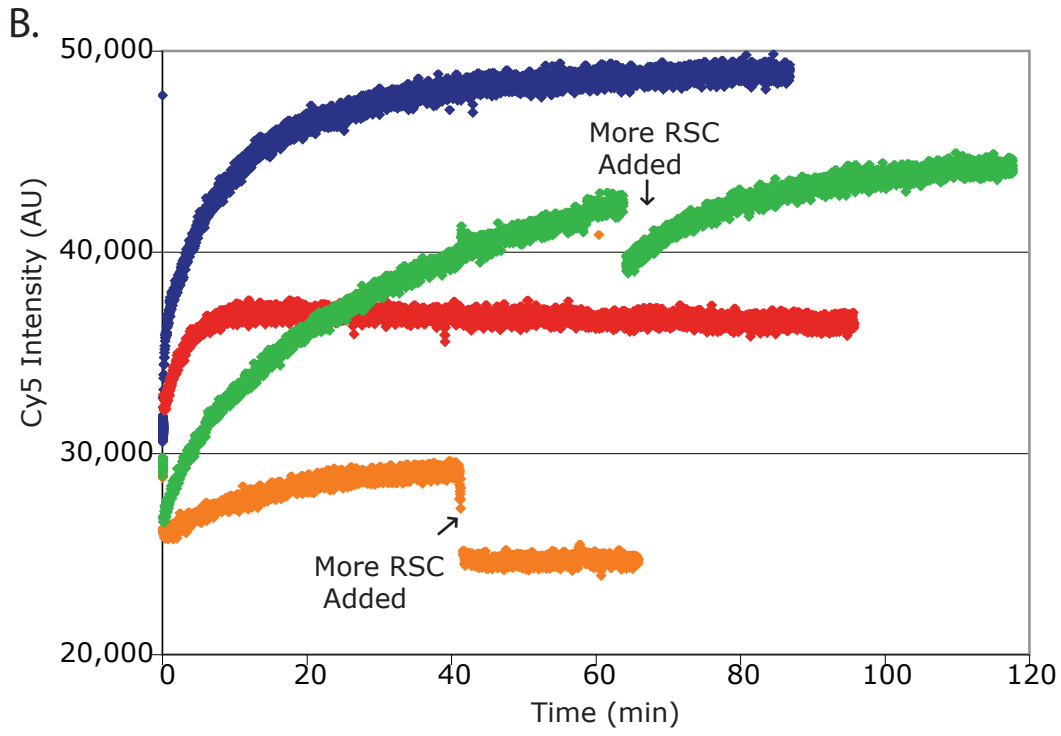
B.
50,000
40,000
30,000
20,000
Cy5 Intensity (AU)
More RSC Added
More RSC Added
0
20
40
60
80
100
120
Time (min)

Figure 5:

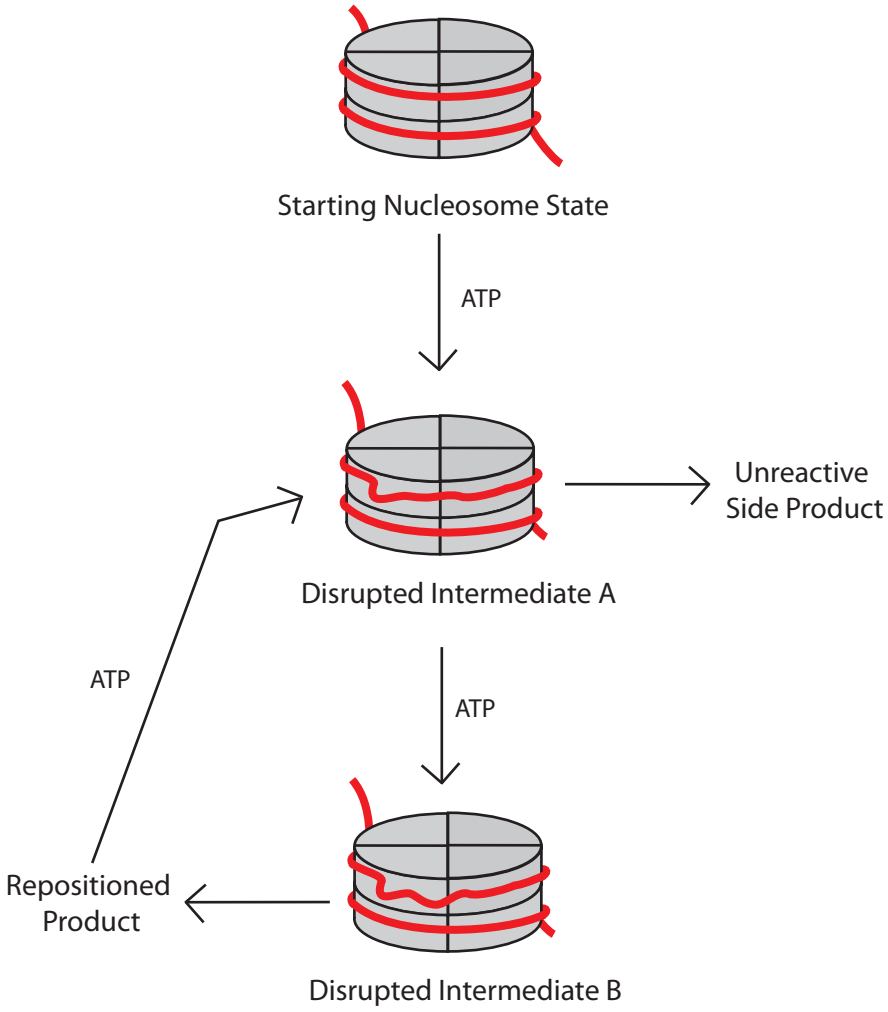
Starting Nucleosome State
ATP
Unreactive
Side Product
Disrupted Intermediate A
ATP
ATP
Repositioned
Product
Disrupted Intermediate B

Figure 6:

A. Nucleosomes

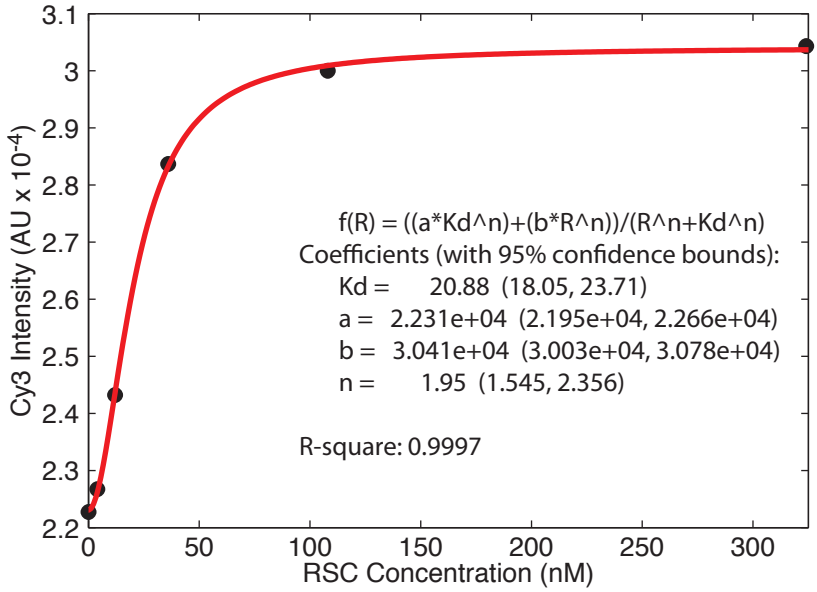

B. DNA

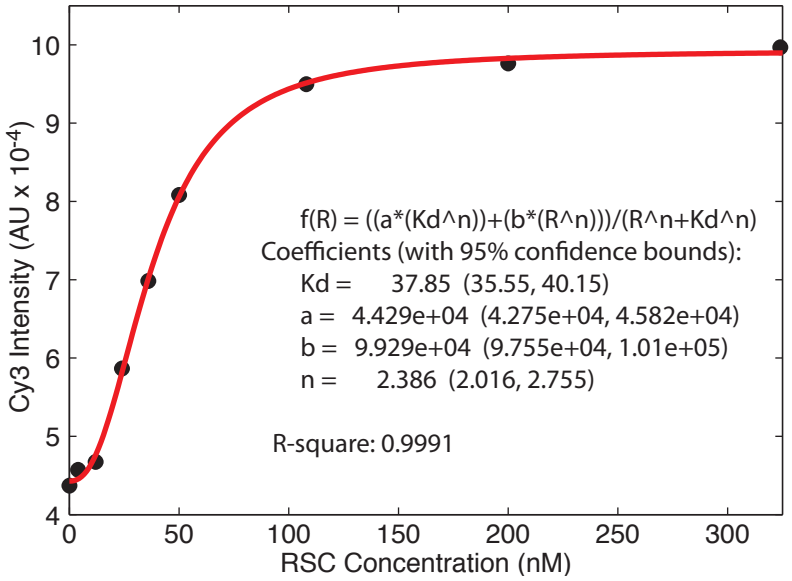

Figure 7:

A.

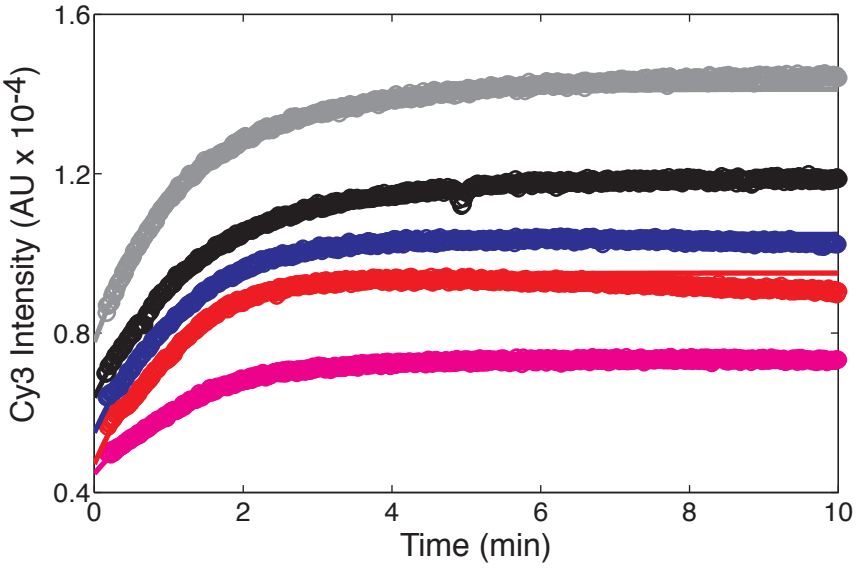
1.6
1.2
0.8
0.4
Cy3 Intensity (AU x 10-4)
0
2
4
6
8
10
Time (min)

B.

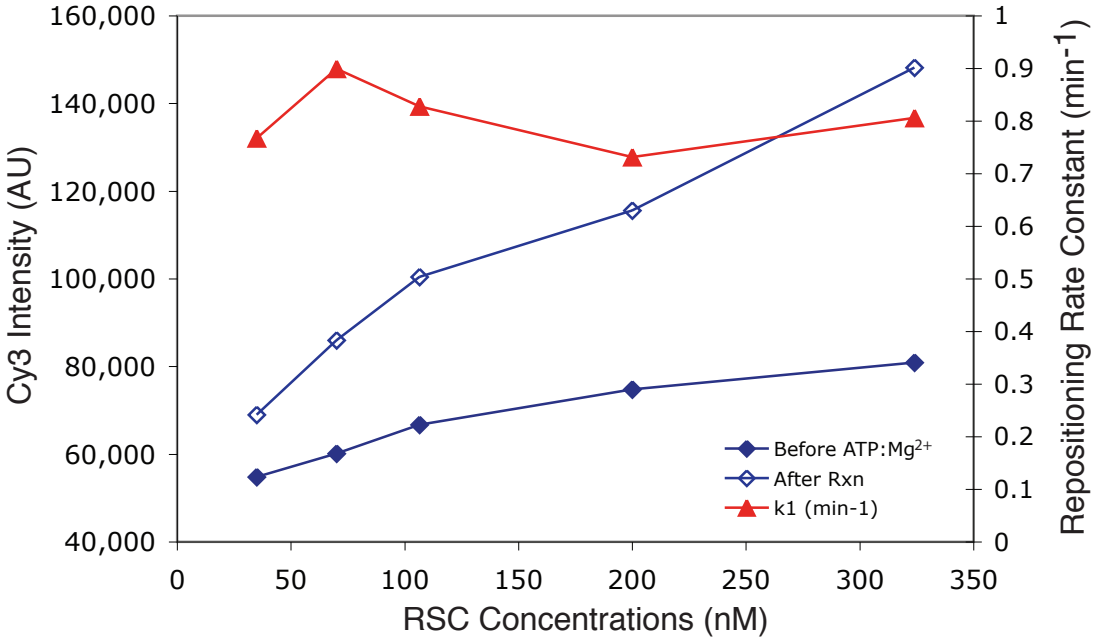
160,000
140,000
120,000
100,000
80,000
60,000
40,000
Cy3 Intensity (AU)
1
0.9
0.8
0.7
0.6
0.5
0.4
0.3
0.2
0.1
0
Repositioning Rate Constant (min-1)
0
50
100
150
200
250
300
350
RSC Concentrations (nM)
Before ATP:Mg2+
After Rxn
k1 (min-1)

Publishing Agreement

It is the policy of the University to encourage the distribution of all theses, dissertations, and manuscripts. Copies of all UCSF theses, dissertations, and manuscripts will be routed to the library via the Graduate Division. The library will make all theses, dissertations, and manuscripts accessible to the public and will preserve these to the best of their abilities, in perpetuity.

Please sign the following statement:

I hereby grant permission to the Graduate Division of the University of California, San Francisco to release copies of my thesis, dissertation, or manuscript to the Campus Library to provide access and preservation, in whole or in part, in perpetuity.

Claire Rowe
Author Signature

3/23/10
Date